Applied Catalysis B: Environmental 254 (2019) 500–509

Contents lists available at ScienceDirect

Applied Catalysis B: Environmental

journal homepage: www.elsevier.com/locate/apcatb

The development of new pigments: Colorful g-C_3N_4-based catalysts for nicotine removal

Shujun Chen[a], Wangyang Lu[a,*], Haibin Shen[a], Shasha Xu[a], Xia Chen[a], Tiefeng Xu[a], Yu Wang[a], Yi Chen[a], Yan Gu[a], Chun Wang[a], Xiao-Feng Wu[b], Matthias Beller[b], Wenxing Chen[a,*]

[a] National Engineering Lab for Textile Fiber Materials & Processing Technology (Zhejiang), Zhejiang Sci-Tech University, Hangzhou, 310018, China
[b] Leibniz-Institut für Katalyse e.V. an der Universität Rostock, Albert-Einstein-Straße 29a, 18059, Rostock, Germany

ARTICLE INFO

Keywords:
g-C_3N_4
Colorful catalysts
Pigments
Nicotine

ABSTRACT

The comfortable, beautiful and healthy residential environment has been a target pursued by human beings. However, the inevitable presences of indoor air pollutants such as nicotine which release from tobacco smoking imperceptibly invade people's health. Here, we developed new pigments consisted by colorful graphitic carbon nitride (g-C_3N_4)-based catalysts, which were fabricated by facile calcining and water bath refluxing procedures. The catalytic pigments exhibited a high catalytic activity for the removal of nicotine under sunlight or even light emitting diode (LED). The designed experiments revealed that superoxide radicals ($^{\cdot}O_2^-$) were main active species in g-C_3N_4-based catalysts system and played a significant role in removing contaminants. Noteworthy, the catalysts as pigments were successfully used for coloring textiles and painting. Both the catalytic textiles and paintings were provided with preferably photocatalytic performance and reusability. The catalytic pigments were simple to prepare, brightly colored and could effectively degrade nicotine, thus not only have decorative effect, enriching the spiritual world, but also contribute to the protection of the environment of human life.

1. Introduction

With the development of both economy and civilization in human society, human's living standards and decoration tastes are increasing. For our own health concerning, more and more people begin to put forward on green and healthy dwelling environment [1]. However, the complicated environmental pollutions such as tobacco smoking [2–4], benzenes [5,6], formaldehyde [7,8], and even bacterial infections have led to massive health loss [9,10]. For instance, nicotine that derives from tobacco smoking has been accepted as a well-known source of primary indoor air pollutants [11]. As a semi-volatile organic pollutant, it has a strong surface adhesion and can easily remain on the surface of walls, curtains and carpets, which may imperceptibly cause cancer or other diseases in families, especially serious for children [12–14]. Since most people spend approximately 90% of time indoor, the indoor air quality is extremely important for public health [15]. How to effectively purify the indoor contamination to possess a safe and comfortable living environment is a big challenge for human beings [16].

In residential environment, pigments as fundamental materials of art are indispensable parts of indoor landscaping and decoration. They are widely used in wall ornament, art crafts, textile printing and dyeing. The development of pigments can be trace back to long time ago [17], that ancient people used natural pigments derived from roots, berries, leaves, minerals, and even crushed insects to decorate their life. With time, people discovered and created a large number of metallic, inorganic and organic pigments [18,19]. Until now, people are still exploring new functional pigments. However, these classic pigments in our daily life only have the function of decoration. It is more subversive to develop novel pigments that they can directly removing indoor harmful substance in addition to adornment.

Theoretically, the color of pigments is the result of the absorption and release of different light wavelengths [20]. In the field of catalysis, photocatalysts just like most pigments can also absorb light and exhibit different colors. Admittedly, the difference from pigments is that photocatalysts can also excite photoelectrons after absorbing a sufficient amount of light energy to generate high reactive species and holes [21,22], allowing their application in different chemical processes such as hydrogen production, decomposition of organic pollutants, air purification [23,24], mildew prevention, and sterilization [25–31]. Methods such as noble metal deposition, metal/non-metal doping, dye-sensitizing and semiconductor compositing on catalysts can facilitate the transfer of electrons to develop various photocatalytic systems

* Corresponding authors.
E-mail addresses: luwy@zstu.edu.cn (W. Lu), wxchen@zstu.edu.cn (W. Chen).

https://doi.org/10.1016/j.apcatb.2019.05.023
Received 17 January 2019; Received in revised form 28 April 2019; Accepted 5 May 2019
Available online 06 May 2019
0926-3373/

[32–35]. In the field of materials and chemical engineering, however, research has seldom concentrated on the aspect of catalyst color, and most photocatalysts are monotonous and unaesthetic. Thus, some questions need to be considered when colorful catalysts are used as pigments, such as endowing monotonous photocatalysts more beautiful colors and high photocatalytic activity under visible light, loading the powder catalytic pigments on the substrates firmly, and avoiding the oxidation corrosion of substrate materials, that usually occurs in hydroxyl radical (˙OH) dominated catalytic system [36,38].

Here, we used a two-dimensional graphitic carbon nitride (g-C_3N_4) nanosheet catalyst to synthesize multi-colored catalytic pigments. The nanosheet had a polymeric structure that easily allowed it to change its structure and catalytic activity through molecular modification and surface engineering [38–40]. The colorful g-C_3N_4-based catalytic pigments have great photocatalytic performance towards the nicotine removal under sunlight or even light emitting diode (LED) irradiation, and the non-˙OH dominated mechanisms of colorful g-C_3N_4-based catalytic pigments are proposed. Furthermore, the catalytic pigments could be firmly colored on the common indoor materials such as textiles and papers through organic thermal bonding or inorganic chemical bonding methods, endowing the indoor materials both the aesthetics of art and the functionality to decontamination.

2. Experimental

2.1. Materials and reagents

LMP/R textiles were processed by Ningbo Aotexun Co., Ltd. (Zhejiang, China). Nano Fe_2O_3 was purchased from Aladdin Reagent (Shanghai, China). Nicotine was obtained from J&K Scientific (Shanghai, China). Phthalocyanine (FePc) was supplied by Tokyo Chemical Industry Co. i. TD. Graphene nanoplatelets (GR) (6–8 nm thick × 5 μm wide) and silica gel (8–15 nm) were obtained from Strem Chemicals Inc (USA) and Jinghuo Co., Ltd. (Shandong, China), respectively. Hexadecachloroferricphthalocyanine ($FePcCl_{16}$) was synthesized according to a procedure previously reported literature [41]. All other chemicals were of analytical grade and were used without further purification.

2.2. Catalyst preparation

2.2.1. Preparation of catalytic pigments

The preparation of catalytic pigments is shown in Scheme 1. g-C_3N_4 synthesis was according to the typical synthesis process [42]. Urea (20 g) was placed in a crucible covered with tin foil paper heated to 550 °C at a rate of 2.5 °C/min and kept at the high temperature for 2 h. The resulting little yellow catalysts were cooled at room temperature and then subjected to an ultrasonic stripping treatment. g-C_3N_4/FePc, g-C_3N_4/$FePcCl_{16}$, g-C_3N_4/Fe_2O_3 can be obtained as follows: 1000 mg g-C_3N_4 was dispersed in N, N'-dimethylformamide (DMF) by ultrasonic treatment for 30 min and then kept in a water bath at 90 °C for 45 min. Meanwhile, the required amount of FePc was sonicated in DMF for 30 min. and then poured into above-mentioned water bath to mix with g-C_3N_4 for 6 h. The preparation of g-C_3N_4/$FePcCl_{16}$, g-C_3N_4/Fe_2O_3 was carried out following the same procedure described for g-C_3N_4/FePc, with the only difference being that FePc was replaced by $FePcCl_{16}$ or Fe_2O_3. The feed ratios of FePc, $FePcCl_{16}$, and Fe_2O_3 were 15.5%, 9.5% and 15.5%, respectively. g-C_3N_4/GR was obtained by a simple calcination method. Specifically, a mixture of 20 g urea and 200 mg graphene was plated into a covered crucible and the heating process is the same as g-C_3N_4. The obtained gray powders were then treated with ultrasonic stripping. The organic elemental analysis was used to determine the mass fraction of GR in g-C_3N_4/GR (Table S1) with a value of 5.6% was obtained.

2.2.2. Preparation of colored catalytic textiles

As shown in Fig. S1, the prepared LMP/R was first placed into the g-C_3N_4, g-C_3N_4/FePc, g-C_3N_4/$FePcCl_{16}$, g-C_3N_4/Fe_2O_3 and g-C_3N_4/GR catalytic pigments. The catalytic textiles were obtained by dip-padding the catalyst suspension (double-dip-double-nip) and pre-heating at 140 °C for 30 min. Later, the pre-heated textiles were hot-pressed at 100 °C for 30 s. The five colored catalytic textiles were named Y-LMP/R, B-LMP/R, G-LMP/R, R-LMP/R, GR-LMP/R, respectively. According to the difference of quality before and after textile loading, the amount of catalytic pigments on textiles was approximately 3%.

2.2.3. Preparation of catalytic paintings

First, the five colored catalytic pigments (g-C_3N_4, g-C_3N_4/FePc, g-C_3N_4/$FePcCl_{16}$, g-C_3N_4/Fe_2O_3 and g-C_3N_4/GR: 10 mg, respectively) were mixed with 10% SiO_2 gel, and treated with ultrasound for 30 min, then drew on the hot-pressed LMP/R textiles (2 cm × 7 cm). Last, the paintings were heated at 50 °C for 30 min.

2.3. Photocatalytic experiments

To assess the photocatalytic performance of catalytic pigments, nicotine was selected as the model substrate. The experiment was conducted in a 40 ml glass beaker under solar irradiation delivered by a Q-Sun Xe-1 test chamber (USA) or commercial white LED (20 W). Before irradiation catalytic pigments (0.1 g/L) was dispersed in nicotine aqueous solution (5 mg/L) and treated by sonication. At given time intervals, the concentration of nicotine was analyzed by ultra-performance liquid chromatography.

To investigate the photocatalytic activity of nicotine by catalytic textiles, catalytic textiles (2 cm × 2 cm) were directly put under light irradiation after adsorbed a certain amount of nicotine (20 μg). The residue nicotine on catalytic textiles was eluted by NaOH aqueous solution and then detected by UPLC/Synapt G2-S HDMS (Waters Q-TOF, USA) analyses.

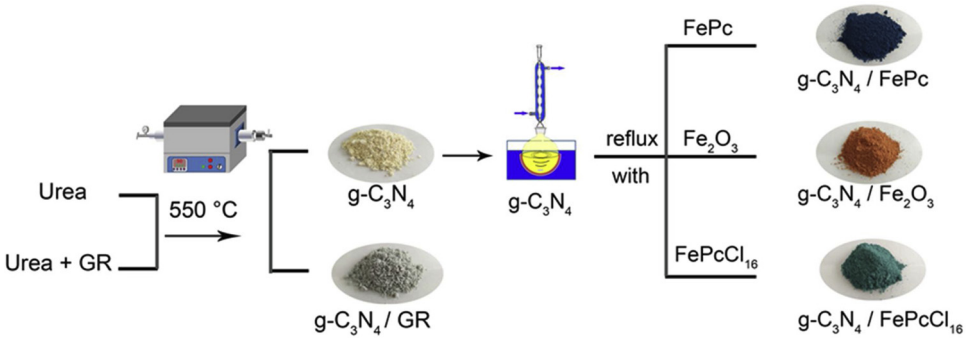

Scheme 1. Synthesis of colorful g-C_3N_4-based catalysts.

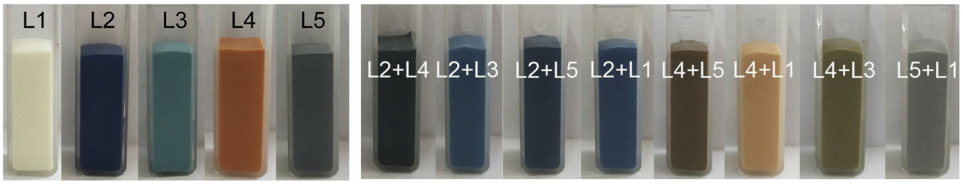

Fig. 1. Visual appearance of catalyst suspensions and color modulation between them. (L1) g-C_3N_4, (L2) g-C_3N_4/FePc, (L3) g-C_3N_4/$FePcCl_{16}$, (L4) g-C_3N_4/Fe_2O_3 and (L5) g-C_3N_4/GR.

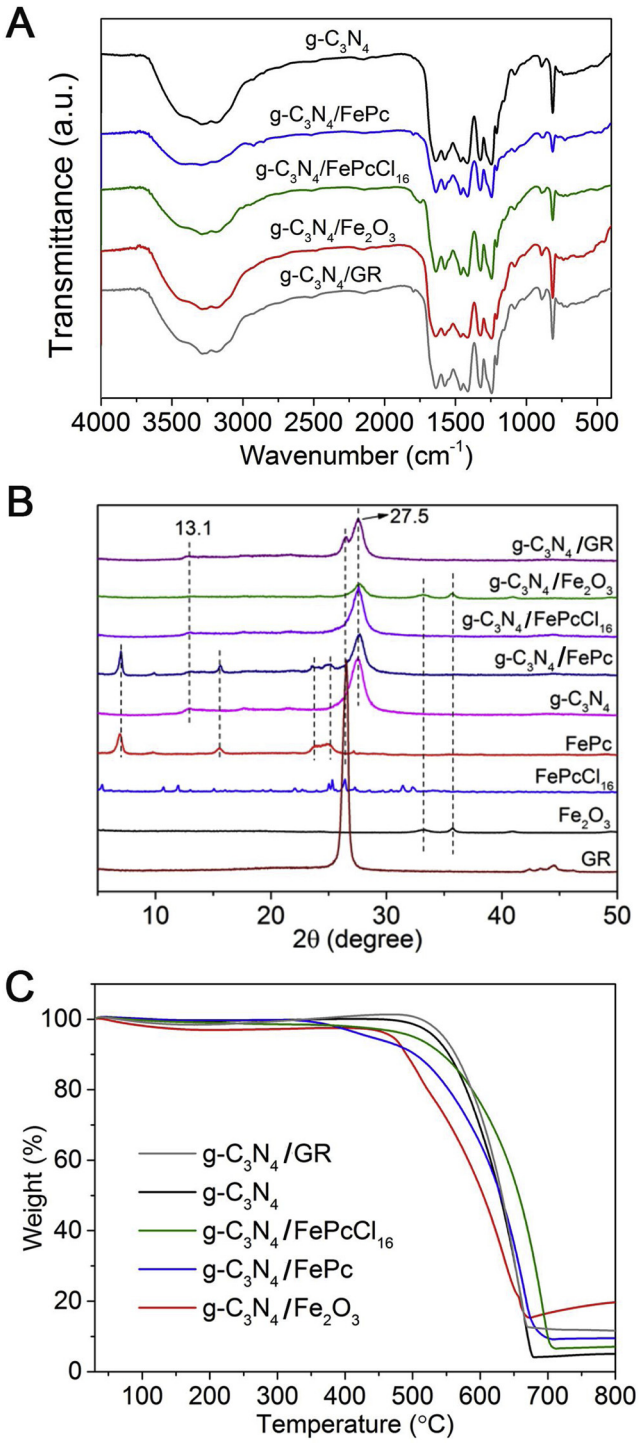

Fig. 2. Structural characterization of catalytic pigments. (A) FT-IR spectra; (B) XRD; (C) TGA.

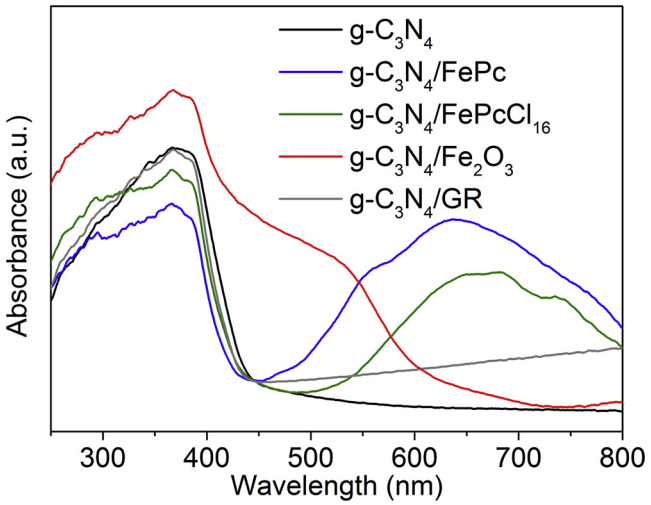

Fig. 3. UV–vis diffuse reflectance absorption spectra of catalytic pigments.

2.4. Analytical methods

The characteristic structure of catalytic pigments were detected by Fourier-transform infrared spectroscopy spectra (FT-IR, Thermo Nicolet 5700), X-ray diffraction (XRD, DX-2700) with Cu-Kαradiation, and thermogravimetric analysis (TGA, Mettler Toledo) carried out from 30 to 800 °C at 20 °C/min in nitrogen atmosphere. The UV–vis diffused reflectance spectra (DRS) of the samples were measured by Lambda 900 UV–vis spectrometer (Perkin Elmer, USA). Electron paramagnetic resonance (EPR) signals were conducted in a Bruker A300 spectrometer (Bruker, Germany) at room temperature. The instrument parameters are set as follows: the central field: 3480 G, the microwave frequency: 9.77 GHz, the modulation frequency: 100 kHz, and the power: 20.00 mW. UPLC/Synapt G2-S HDMS (Waters Q-TOF, USA) in positive mode was used to analyze intermediates in nicotine degradation.

3. Results and discussion

3.1. Characterization

Fig. 1 shows the visual appearance of catalyst suspensions. The little yellow g-C_3N_4 (L1) was changed to blue (L2), green (L3), brick-red (L4), and gray (L5), when it combined with FePc, $FePcCl_{16}$, Fe_2O_3 and GR, respectively. Furthermore, by mixing above five colored catalysts, more different hues of catalysts could be obtained, which could satisfy the basic aesthetic needs of people. The characteristic structure of catalytic pigments was analyzed by FT-IR spectroscopy (Figs. 2A and S2). As shown in Fig. S2, the representative peaks appearing at 1295, 1140, and 1080 cm^{-1} for the phthalocyanine compounds can be assigned to the C–N in pyrrole stretching vibration, and the band at 769 cm^{-1} is ascribed to the N—Fe—N angle changing and stretch vibrations [41,43]. A strong absorption band around 439 and 524 cm^{-1} of Fe_2O_3 were due to Fe—O vibration mode [44]. In Fig. 2A, the original g-C_3N_4 exhibited characteristic absorption peaks similar to those in the previous literature [39,42]. The broad absorption bands between 3300 and 3100 cm^{-1} mainly due to the uncondensed amine groups and intermolecular hydrogen-bonding interactions. The bands in the range

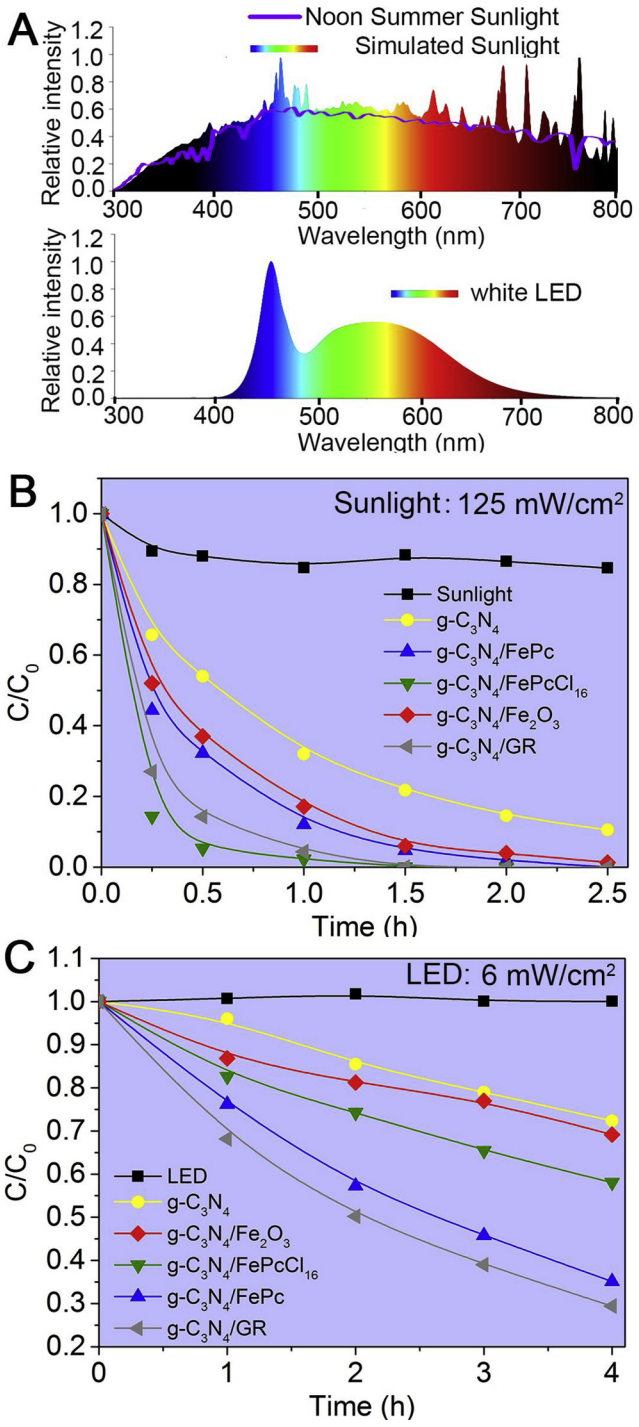

Fig. 4. (A) Sunlight and white LED spectra. (B and C) Photocatalytic degradation of nicotine in the presence of five catalytic pigments under simulated sunlight and white LED irradiation. [g-C_3N_4, g-C_3N_4/FePc, g-C_3N_4/$FePcCl_{16}$, g-C_3N_4/Fe_2O_3 and g-C_3N_4/GR: 0.1 g/L, respectively; nicotine: 5 mg/L].

between 1600–1200 cm^{-1} were ascribed to the typical vibrations of aromatic carbon nitride heterocycles and the characteristic bands at 880–800 cm^{-1} were assignable to the triazine units [45,46]. Furthermore, the multiple peaks of g-C_3N_4, g-C_3N_4/FePc, g-C_3N_4/$FePcCl_{16}$, g-C_3N_4/Fe_2O_3 and g-C_3N_4/GR remain almost unchanged, which suggests that the bulk structure and chemical skeleton of g-C_3N_4 have not been severely altered. However it is difficult to find the typical signal peaks of phthalocyanine compounds or ferric oxide additives in g-C_3N_4-based catalytic pigments. This is mainly due to the strong absorption peaks of

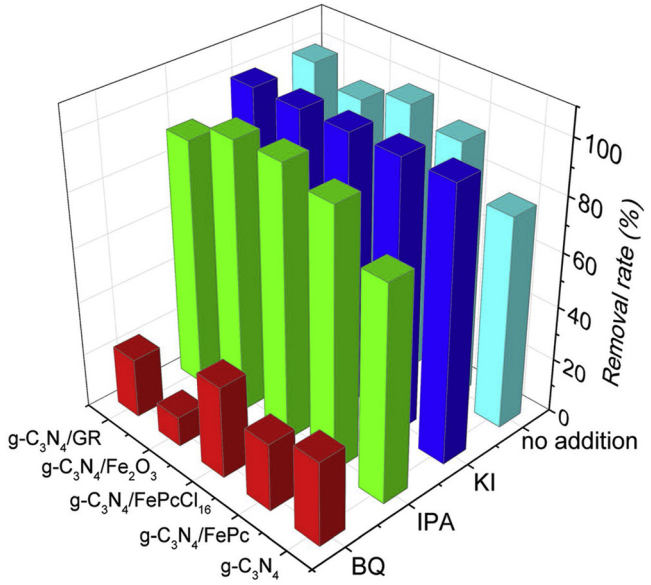

Fig. 5. Effect of trapping agents on the photocatalytic degradation of nicotine [g-C_3N_4, g-C_3N_4/FePc, g-C_3N_4/$FePcCl_{16}$, g-C_3N_4/Fe_2O_3 and g-C_3N_4/GR: 0.1 g/L, respectively; nicotine: 5 mg/L; under solar irradiation, 90 min].

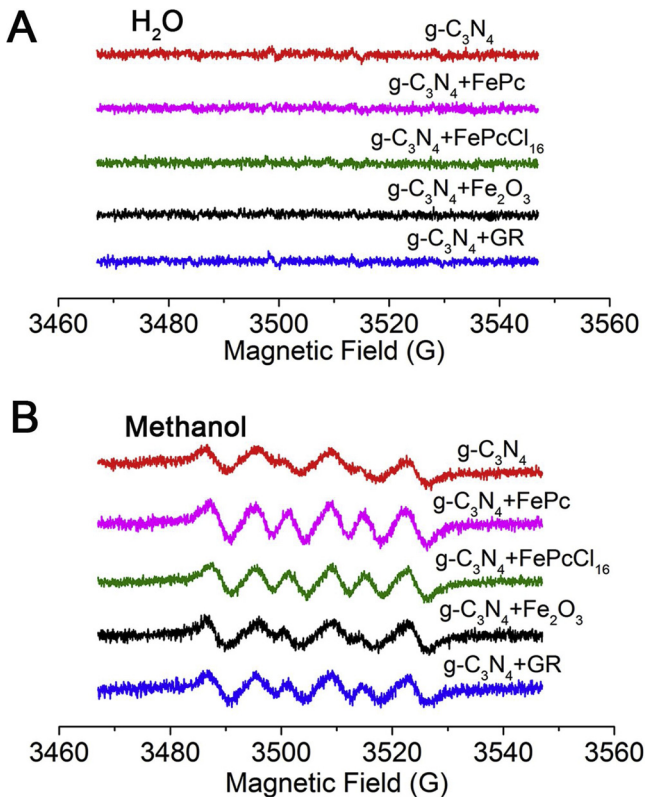

Fig. 6. DMPO spin-trapping EPR spectra in aqueous or methanol solutions in the presence of catalytic pigments under solar irradiation, (A) aqueous solution and (B) methanol solution. [DMPO] = 10 mM.

g-C_3N_4, and the absorption peaks of phthalocyanine compounds were covered by g-C_3N_4. XRD patterns of the samples are presented in Fig. 2B. All as-prepared catalysts showed two peaks at 13.1° and 27.4° corresponding to (100) and (002) crystal planes, indicating g-C_3N_4 still retained the intrinsic structure after modified [47,48]. And multi-colored g-C_3N_4-based catalysts also exhibit characteristic diffraction peaks for the corresponding additive. That mean colorful binary

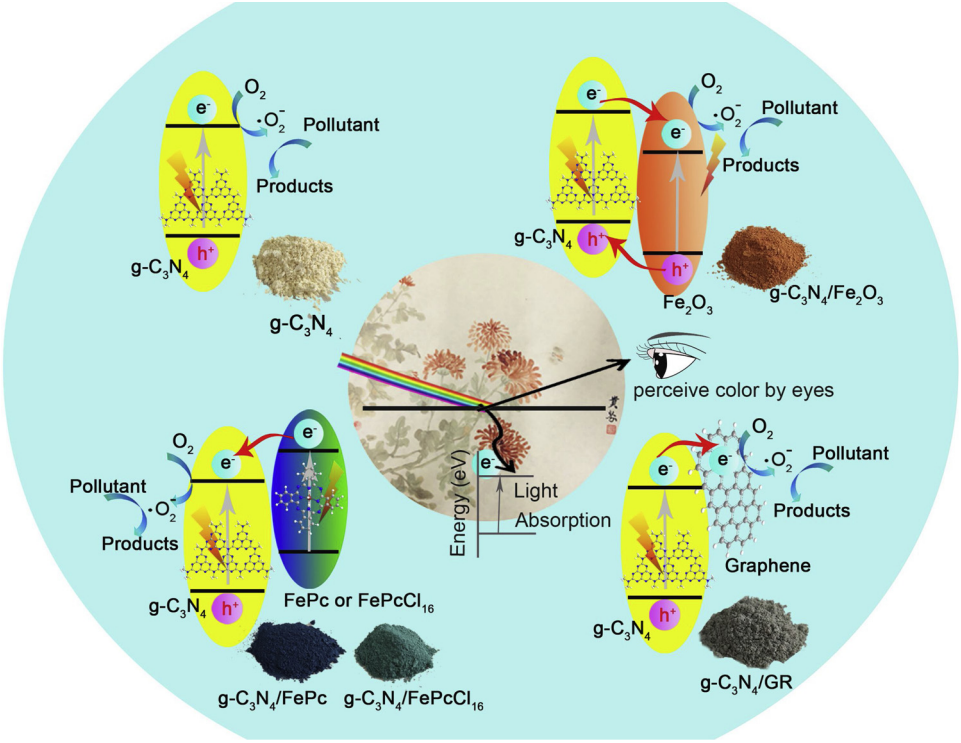

Fig. 7. Possible mechanism of photocatalytic degradation by catalytic pigments.

composite catalysts did not alter diffraction peak position of single composition, and each component is mutually independent. The diffraction peaks of $FePcCl_{16}$ in g-C_3N_4/$FePcCl_{16}$ commixtures weren't observed because of the low amount and fairly low diffraction intensity of $FePcCl_{16}$ on the surfaces of g-C_3N_4. Moreover, these g-C_3N_4-based catalysts exhibited high thermal stability up to 350 °C, and g-C_3N_4/GR was even stable at 500 °C (Fig. 2C), indicating that these catalytic pigments with a high temperature resistance could be employed in relatively high-temperature applications. And the residues of binary composite catalysts were all higher than pure g-C_3N_4, which also indicated FePc, $FePcCl_{16}$, Fe_2O_3 and GR were successfully combined with g-C_3N_4. The optical absorption properties of catalytic pigments were studied by UV–vis DRS. As can be seen in Fig. 3, pristine g-C_3N_4 showed the absorption edge around 450 nm, which mean it only used limited visible light [49], whereas the colorful binary composite catalysts exhibited intense and excellent visible light absorption properties. The absorption and release of light at different wavelengths can make the catalysts present different colors; on the other hand, the wider visible light absorption is also conducive to the photocatalytic reaction. Furthermore, the UV–vis spectrum of strict physical mixture of the components (g-C_3N_4 + FePc, g-C_3N_4 + $FePcCl_{16}$, g-C_3N_4 + Fe_2O_3 and g-C_3N_4 + GR) were also presented in Fig. S3. Obviously, the as-prepared catalytic pigments that prepared by reflus method exhibited a stronger absorption peak than those just by physical mixture in the visible light region, and had more uniform and bright colors.

3.2. Photocatalytic activity and mechanism analysis of catalytic pigments

3.2.1. Photocatalytic activity

Sunlight and LED are two common lights in our daily life. Fig. 4A shows simulated sunlight and commercial white LED spectra. In nature, the solar spectrum includes ultraviolet, visible and infrared regions, while the light-emitting diode (LED) in daily indoor environment only has visible light spectrum, from 400 to 800 nm. Therefore, the catalysts have great different activity under solar and LED irradiation. In our experiments, the spectra power distribution of simulated sunlight providing by a Q-Sun xenon test chamber Q-SUN Xe-1 is similar to the noon summer sunlight. First, we detected photocatalytic degradation of nicotine in the presence of FePc, $FePcCl_{16}$, Fe_2O_3 and GR additives under sunlight. In Fig. S4, the concentration of nicotine showed no obvious change in the presence of solar irradiation without g-C_3N_4, which indicates g-C_3N_4 plays a significant role in this catalytic pigment system. Under the simulated solar irradiation, with 125 mW/cm^2 optical power density, all the colorful catalysts including g-C_3N_4 had a high activity towards the degradation of the nicotine (Fig. 4B). After the sunlight irradiation for 2.5 h, the removal rate of nicotine by yellow g-C_3N_4 reached around 90%, while nearly 100% of nicotine had been removed by other colorful binary composite pigments. In Fig. 4C, under the low optical power density of commercial LED (6 mW/cm^2), it was more obviously to see that the colorful binary composite catalysts had higher photocatalytic activity than pure g-C_3N_4 because of their wider absorbing range of wavelengths. The fast gray g-C_3N_4/GR could degrade over 70% nicotine under white LED for 4 h.

3.2.2. Mechanism analysis

To better understand the possible catalytic mechanism of colorful catalysts, trapping experiments of radicals and spin-trapping electron paramagnetic resonance (EPR) were performed, as shown in Fig. 5. The capture agents, such as benzoquinone (BQ), isopropanol (IPA) and potassium iodide (KI), were applied to observe the effect on the photocatalytic efficiency of nicotine [50–52]. All the nicotine degradation was greatly suppressed by the addition of BQ, indicating that the superoxide radicals ($^{\cdot}O_2^-$) were mainly responsible for the photocatalytic response [53]. When KI was added into the reaction system, the removal rate was generally faster than no addition. That's mainly because KI as the holes (h^+) scavenger prevents the recombination of photoelectrons and holes, so that promoting the generating of $^{\cdot}O_2^-$. On the other hand, the remove rate of nicotine had no obvious decrease with the existence of IPA. Thus, $^{\cdot}OH$ was not the main active species in our catalytic pigment systems [37]. The results were in good consistent with the EPR test. In Fig. 6A and B, the clear signals of DMPO-$^{\cdot}O_2^-$ were detected in methanol after 100 s of light exposure, while no

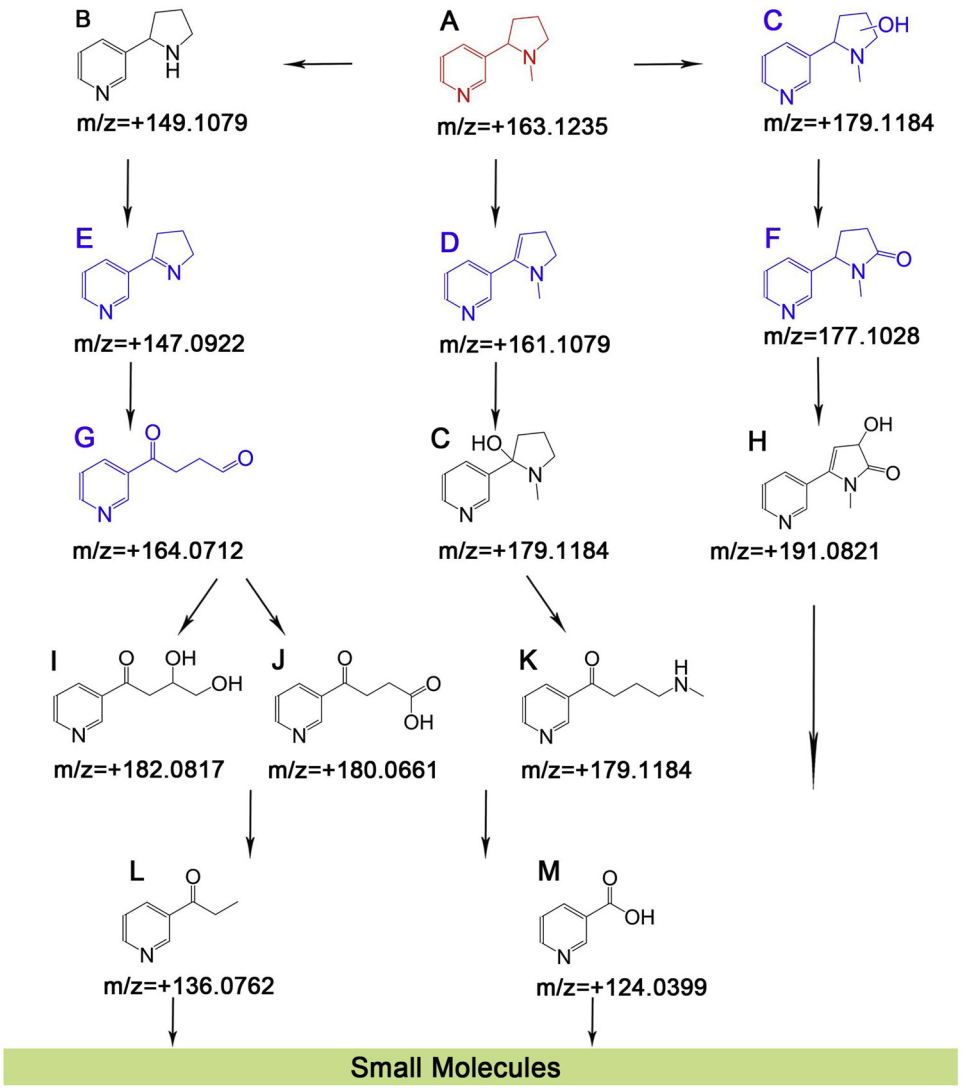

Fig. 8. Possible degradation pathway of nicotine over g-C_3N_4/GR catalyst under solar irradiation.

obvious signal of DMPO-˙OH could be obtained in aqueous solution [54,55].

According to above experiments, the possible photocatalytic mechanism of these catalytic pigments were proposed in Fig. 7. For g-C_3N_4/FePc and g-C_3N_4/$FePcCl_{16}$, the electrons produced on the excited phthalocyanine molecule were transferred to the conduction band of g-C_3N_4, accelerating the formation of $^{\cdot}O_2^-$ and favoring the degradation of the organic pollutant. For g-C_3N_4/Fe_2O_3 and g-C_3N_4/GR, the introduction of Fe_2O_3 and GR promoted the interfacial electron transfer process, reducing the probability of electron-hole recombination, which also facilitated the production of $^{\cdot}O_2^-$. The photocatalytic behavior of the colorful g-C_3N_4-based catalysts, dominated by the action of $^{\cdot}O_2^-$, was different from that of traditional TiO_2-based systems, dominated by the effect of the ˙OH. As a consequence, the corrosion of organic supporter could be effectively avoided [36,37]. Inset picture in Fig. 7 shows that when different wavelengths light radiate on the painting (painted with catalytic pigments), the excited electrons by light energy can transfer to the surface of pigments and then combine with O_2 in air to generate active $^{\cdot}O_2^-$. Meanwhile the reflected light is interpreted by our brain as a particular color. Thus, the dual functionality of decontamination and decoration of pigments is realized.

3.3. Nicotine degradation pathway

In the process of identifying the possible photocatalytic degradation pathway of nicotine, ultra-performance liquid chromatography and high-definition mass spectrometry was used to analyse the reaction intermediates and thirteen chemicals were detected, which were listed in Table S2. The possible degradation pathway of nicotine was proposed in Fig. 8. The active site of nicotine was the pyrrolidine ring, which was opened during the reaction. The reaction process included demethylation, hydroxylation and dehydrogenation [56], forming intermediates **B–D**, respectively, which were similar to the process of nicotine degradation by microorganisms, including: pyridine pathway, pyrrole pathway and demethylation pathway [57,58]. The intermediate **B** was followed by dehydrogenation, which led to the formation of chemical **E**, and after the loss of the amino group and the ring opening, the intermediate **G** was generated. Hydroxynicotine (intermediate **C**) is oxidized to cotinine (intermediate **F**). Cotinine was further hydroxylated to intermediate **H**. In the dehydrogenation process, intermediate **D** was hydroxylated and then the ring opening forming the ketonic acid (intermediate **K**), finally nicotinic acid (intermediate **M**) is formed. Fig. S5(A and B) show the transformation products (TPs) area profiles as a function of reaction time. The intermediates showed a trend of increasing first and then decreasing. After the reaction completed, no intermediate or small molecular acids were obtained, which

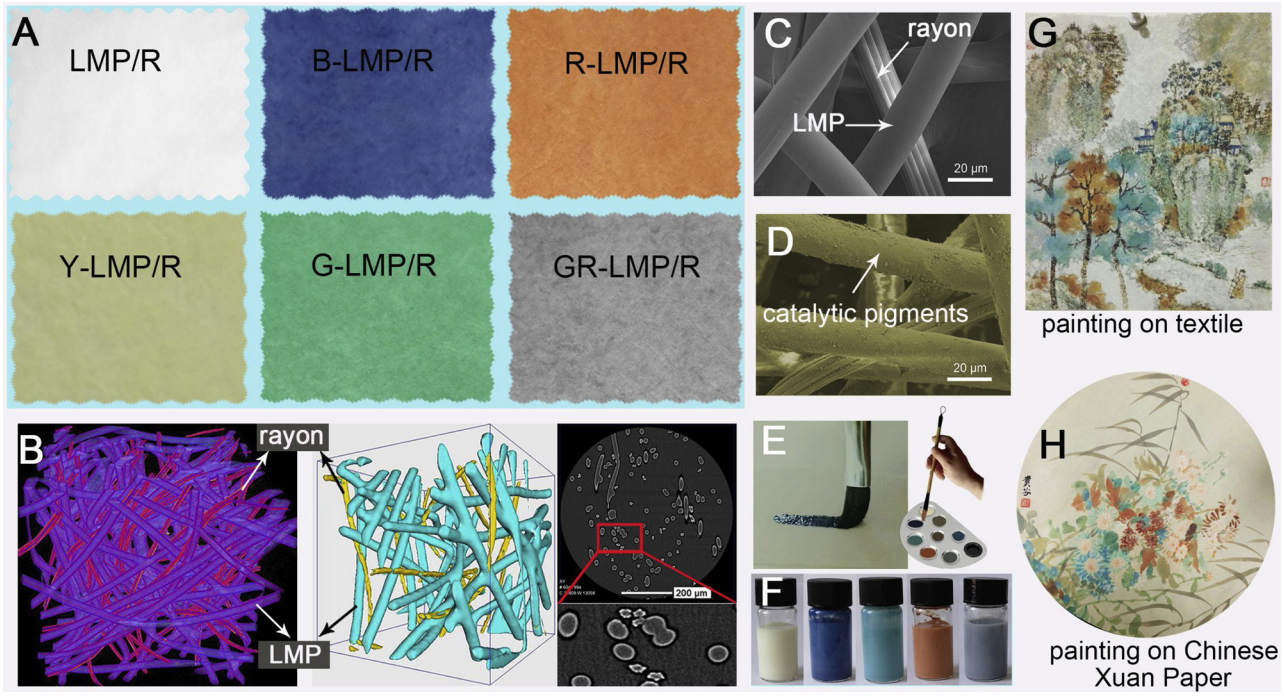

Fig. 9. (A) Photograph of textile stain with catalytic pigments. (B) 3D-XRM of LMP/R textiles (Left: rendering of ZEISS 3D Viewer; middle: ORS segmentation of 3D Viewer; left: 2D slice image). (C) SEM image of LPM/R. (D) SEM image of Y-LPM/R. (E) Schematic illustration of textiles used as canvases in painting. (F) Photograph of catalytic pigments in silica gel. (G and H) Photograph of the finished painting created with catalytic pigments on GR-LMP/R textile and Chinese Xuan Paper.

meant the catalytic pigments were sufficiently powerful to degrade these intermediates and the final products could be mineralized into small molecules like CO_2 and NO_3-. Total organic carbon analyzer (Elementar, Liquid) was used to determine the mineralization rate for the degradation of nicotine. In 30 min, the mineralization rate of g-C_3N_4, g-C_3N_4/FePc, g-C_3N_4/$FePcCl_{16}$, g-C_3N_4/Fe_2O_3 and g-C_3N_4/GR was 4.53%, 5.39%, 6.02%, 6.03%, and 6.18%, respectively, which further indicated the catalytic pigments could gradually mineralize nicotine into carbon dioxide.

3.4. Catalytic pigments used in textiles and paintings

Catalysts with high photocatalytic activity can be applied to fabrics as colorants to produce functional colorful textiles, or mixed with silica gel to produce paint. Currently, polyester (PET) and rayon fibers, the world's largest varieties of synthetic and regenerated fibers, are commonly used in everyday life. Here, the low melting sheath-core composite polyester fiber (LMP) can be used to combine with the g-C_3N_4-based colorful catalysts for producing functional textiles by a hot-melt adhesive process.

Fig. 9A shows that white LMP/R textiles were successfully tinted to yellow (Y-LMP/R), blue (B-LMP/R), green (G-LMP/R), brick-red (R-LMP/R) and grey (GR-LMP/R) via the simple dip-nip and thermal treatment. The microstructural analysis of the fabrics was carried out using 3D X-ray microscopy (XRM), as shown in Fig. 9B. The rendering image clearly shows the distribution of two kinds of fibers: rayon fibers are uniformly dispersed between the LMP fibers, which stick together because the heating treatment caused their fusion. The 2D slice image shows that LMP fibers are circular, while rayon fibers are irregularly shaped. LMP/R textiles with a three-dimensional interpenetrating network can favor the adherence of granular catalytic pigments. Fig. 9C and D show the scanning electron microscopy (SEM) image of white LMP/R and yellow Y-LMP/R textiles. Before coloring, both cylindrical LMP and jagged rayon fibers were smooth and clean. After coloring, the surface of fabrics became rough, suggesting that the yellow g-C_3N_4 catalytic pigments had successfully loaded on the surface of the fabrics (other SEM images of colored textiles in Fig. S6). These catalytic textiles can be used in a wide variety of applications in everyday life, including carpeting, upholstered furnishings, curtains, coverings for tables, walls and other flat surfaces, or in art. Here, we used catalytic textiles as different background painting canvases. In Fig. S7, we can see that original brushy textile was not suitable to paint. Fortunately, the textile became flat and smooth after the hot-pressing procedure. Thus the catalytic textiles also can be used as canvases for painting (Fig. S8).

Fig. 9E shows the use of the blue pigment to draw a line on the textile materials, indicating the possibility of using the catalysts as paints. Generally, the traditional pigments require the addition of a binder such as dextrin, gum, or resin, to ensure their firm adherence to the substrates. However, the organic polymeric adhesives would drastically reduce the activity of the catalytic pigments. Here, the colorless and transparent silica sol with high chemical stability and large surface area wouldn't affect the color of catalytic pigments or their absorption of light. As seen in Fig. 9F, the basic five colors of catalytic pigments in 10% SiO_2 suspension was same as in water. With the evaporation of water, the silica sol firmly adhered to form a silicon-oxygen bond [59]. What's more, the final paintings drawing on GR-LMP/R textile and on traditional Chinese Xuan Paper were exhibited in Fig. 9G and H, respectively. The application of the developed pigments is not limited to these two substrates, but can be extended to woods, walls, ceramics or other flat substrates.

3.5. Catalytic textiles and paintings for nicotine removal

In this work, the catalytic textiles were further tested for the oxidative degradation of nicotine under light irradiation. Fig. 10A shows the removal efficiency of nicotine by the catalytic textiles exposed to solar irradiation. The results showed that about 90% of nicotine adsorbed on the textiles was decomposed by the catalytic pigments within 90 min, whereas 73.1% of nicotine still residue remained on the pure LMP/R textiles, suggesting that the textiles with the colorful catalytic pigments have great photocatalytic activity towards the degradation of nicotine under solar irradiation. In addition to sunlight, the commercial

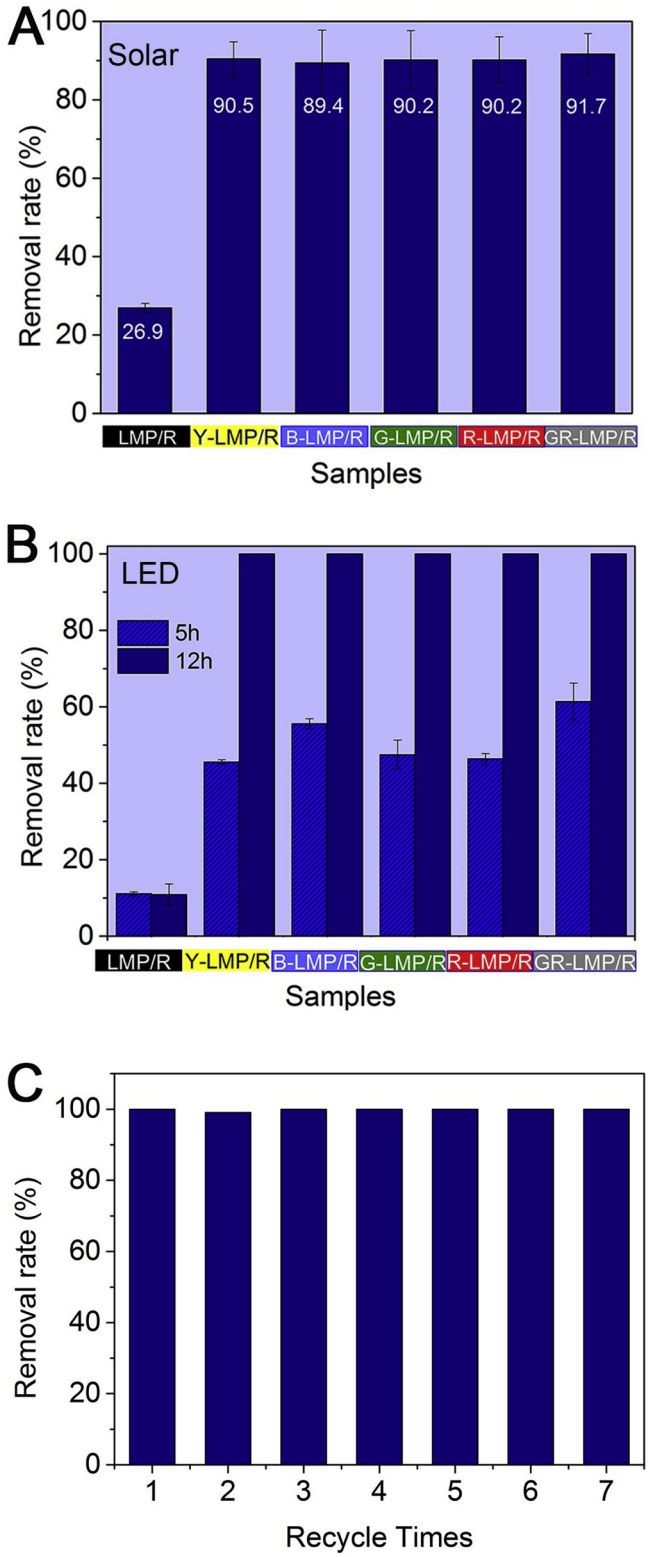

Fig. 10. Photocatalytic degradation of nicotine by colored textiles under (A) sunlight irradiation for 90 min and (B) LED for 12 h [Y-LMP/R, B-LMP/R, G-LMP/R, R-LMP/R, GR-LMP/R: 2 cm × 2 cm, respectively; solar energy density: 125 mW/cm^2; LED energy density: 6 mW/cm^2]. (C) Cyclic potocatalytic degradation of nicotine by GR-LMP/R under sunlight radiation [nicotine: 5 mg/L, size of GR-LMP/R: 2 cm × 7 cm].

LED irradiation with low energy density (6 mW/cm^2) was also used for the photocatalytic degradation of nicotine (Fig. 10B). After 5 h irradiation, about 40%–60% of the nicotine could be removed by the colorful catalytic textiles, and no nicotine was remained on catalytic textiles after 12 h. Thus, the catalytic textiles can also achieve the oxidative degradation of nicotine under indoor mild visible light condition. Furthermore, the results of the photocatalytic cycling tests in the decomposition of nicotine under stimulated sunlight showed that the activity was not reduced after 7 cycles (Fig. 10C). What's more, the FESEM of as-prepared photocatalysts after cyclic photocatalytic reactions have been carried out. As shown in Fig. S9, the surface morphology of the textiles were well maintained and were still rough with some catalysts, which indicate the as-prepared catalytic textiles have excellent load-stability.

On the other hand, for catalytic paintings, the pigments could be stable on the substrate due to the adhesion of silica sol. As shown in Fig. 11A, the colored logo pattern adhered tightly to the textile surface even after it had been dropped in water. The quality of the painting remained intact when it was taken out of the water. The influence of the concentration of adhesive on the photocatalytic activity of the pigment was also discussed in Fig. 11B. With the increase of SiO_2 concentration the degradation of nicotine became faster. Besides, the addition of SiO_2 could help the pigments bonding on the surface of substrates. As can be seen in Fig. 11C, the effluent solution of samples under the low concentration of SiO_2 was turbid after shaking reaction solution, due to the drop of catalytic pigments from the substrate. Considering the pigments need to have both high catalytic activity and strong adhesion to the substrate, 10% SiO_2 was chosen as the binder. Fig. 11D shows the cyclic photocatalytic degradation of nicotine with the catalytic painting drew by grey g-C_3N_4/GR-10%SiO_2 pigments under sunlight irradiation, and the removal rate still maintained over 90% after 7 times recycle, which indicates the catalytic pigments has great stability. Fig. S10 presents the photographs of five colored catalytic paints after sunlight exposure. And the photocatalytic activity of sun-exposed and non-exposed catalytic paints was also compared. The photographs revealed that the color of exposed pigments did not change after light exposure, which also indicates the quality of catalytic pigments is stable.

Based on the experimental results, the possible use of catalytic paintings in the degradation of pollutants is shown in Fig. 12, where g-C_3N_4 was selected as an example. The catalytic pigments on the surface of the substrate are excited by photons, injecting electrons in the conduction band and combining with oxygen in air to form $^{\cdot}O_2^-$, meanwhile, nicotine pollutants adsorbed on the surface of the catalytic pigments are then degraded and removed.

4. Conclusion

In summary, we developed the novel catalytic pigments that not only decorate our rooms with beautiful colors but also own the ability to remove contaminants in residential environment. Excited by light energy, the g-C_3N_4-based catalytic pigments exhibited excellent photocatalytic activity toward nicotine removal under sunlight or even commercial LED irradiation. More importantly, compared to pure g-C_3N_4, the colored g-C_3N_4-based catalysts had a higher photocatalytic activity, because of the improvement of visible absorption by dye sensitization and co-catalyst compositing. Additionally, EPR technology and trapping experiments of radicals revealed that the catalytic pigments presented $^{\cdot}O_2^-$ dominated catalytic mechanism. Furthermore, these catalytic pigments were immobilized on fibers and drew on substrate materials to construct colorful catalytic textiles and painting artworks, which constructed a stable catalytic system and performed great photocatalytic activity to oxidize nicotine under light irradiation. These newly developed pigments show vast potential for application in decoration and painting, which can be drawn into artworks to be exposed in homes or made into wallcoverings to purify the environment in public places such as smoking lounges. Contrarily to traditional pigments, these catalytic pigments with decorative and photocatalytic functions can satisfy both mental and physical health needs.

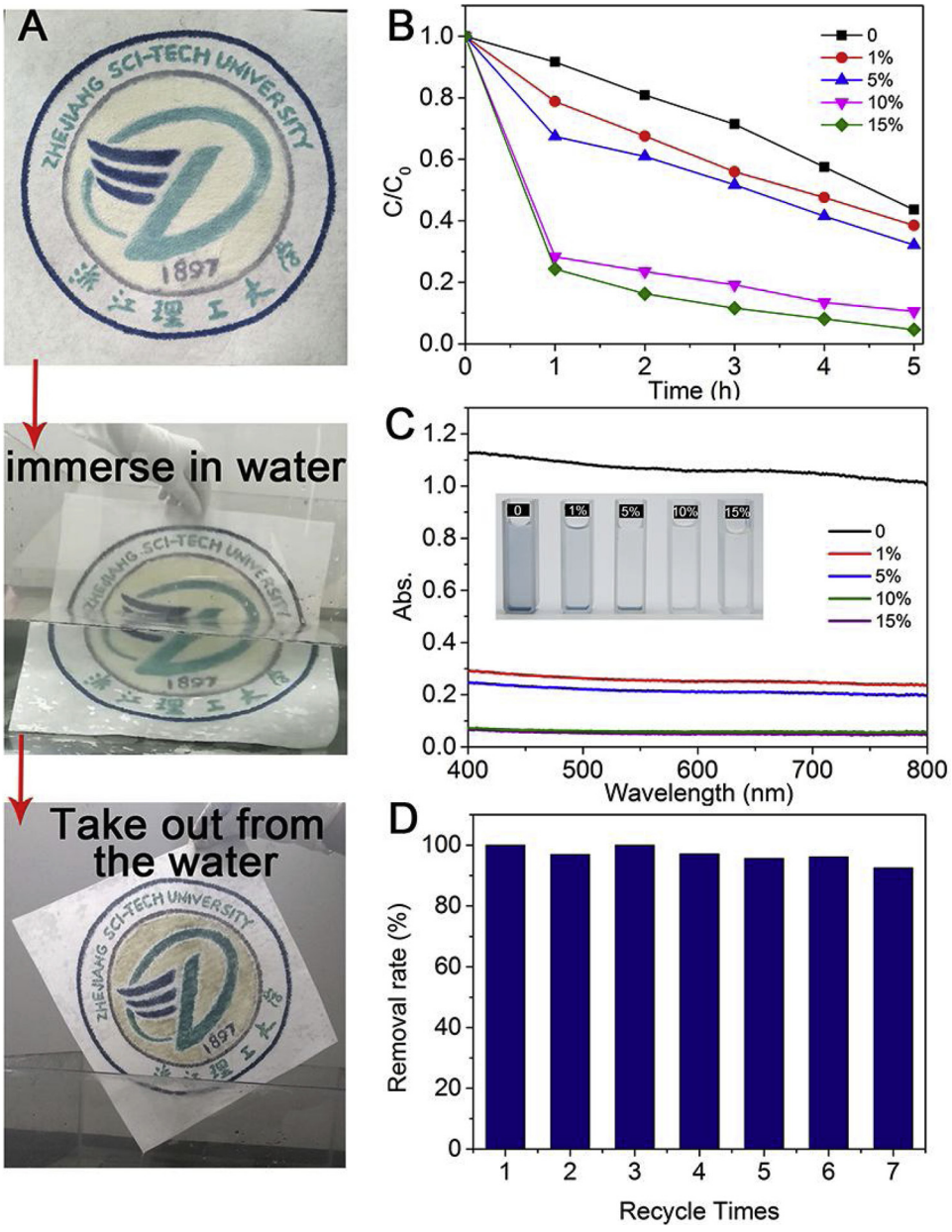

Fig. 11. (A) Painting of the university logo and its stability in water using 10% SiO_2 as a binder. (B) Effect of g-C_3N_4/FePc pigment containing different SiO_2 concentrations on the photocatalytic degradation of nicotine [nicotine: 5 mg/L, size of catalytic painting drew by g-C_3N_4/FePc-10%SiO_2 pigments: 2 cm × 7 cm]. (C) UV–vis absorption spectra of effluent solutions after shaking canvases drew by g-C_3N_4/FePc pigment containing different SiO_2 concentrations. (D) Cyclic photocatalytic degradation of nicotine by catalytic painting under sunlight radiation [nicotine: 5 mg/L, size of catalytic painting drew by g-C_3N_4/GR-10% SiO_2 pigments: 2 cm × 7 cm].

Fig. 12. Possible mechanism for nicotine degradation by catalytic painting and wallcovering.

Author contributions

The manuscript was written through contributions of all authors. All authors have given approval to the final version of the manuscript.

Notes

The authors declare no competing financial interest.

Acknowledgments

The authors thank Chinese outstanding young painter Guifen Bao for the painting, and thank Chenjie Cao (Carl Zeiss Co. Ltd, Shanghai, China) for sample mounting method and imaging technology support in the computed micro-X-ray tomography tests. This research has been supported by the National Natural Science Foundation of China (Nos. 51133006 and 51103133), and Zhejiang Provincial Natural Science Foundation of China (No. LY14E030013).

Appendix A. Supplementary data

Supplementary material related to this article can be found, in the online version, at doi:https://doi.org/10.1016/j.apcatb.2019.05.023.

References

[1] R. Zhang, J.K. Smith, Br. Med. Bull. 68 (2003) 209–225.
[2] F. Fasanelli, L. Baglietto, E. Ponzi, F. Guida, G. Campanella, M. Johansson, K. Grankvist, M. Johansson, M. Assumma, A. Naccarati, M. Chadeau-Hyam, U. Ala, C. Faltus, R. Kaaks, A. Risch, B. De Stavola, A. Hodge, G.G. Giles, M.C. Southey, C.L. Relton, P.C. Haycock, E. Lund, S. Polidoro, T.M. Sandanger, G. Severi, P. Vineis, Nat. Commun. 6 (2015) 10192.
[3] A.J. Sasco, M.B. Secretan, K. Straif, Lung Cancer 45 (Suppl 2) (2004) S3–S9.
[4] L.B. Alexandrov, Y.S. Ju, K. Haase, P.V. Loo, I. Martincorena, S. Nik-Zainal, Y. Totoki, A. Fujimoto, H. Nakagawa, T. Shibata, P.J. Campbell, P. Vineis, D.H. Phillips, M.R. Stratton, Science 354 (2016) 618–622.
[5] R. Andreoli, G. Spatari, D. Pigini, D. Poli, I. Banda, M. Goldoni, M.G. Riccelli, M. Petyx, C. Protano, M. Vitali, M. Barbaro, A. Mutti, Environ. Res. 142 (2015) 264–272.
[6] M.T. Smith, Annu. Rev. Publ. Health 31 (2010) 133–148.
[7] T. Salthammer, S. Mentese, R. Marutzky, Chem. Rev. 110 (2010) 2536–2572.
[8] Z. Xu, J. Yu, M. Jaroniec, Appl. Catal. B 163 (2015) 306–312.
[9] B.F. Yu, Z.B. Hu, M. Liu, H.L. Yang, Q.X. Kong, Y.H. Liu, Int. J. Refrig. 32 (2009) 3–20.
[10] T. Husman, Scand. J. Work Environ. Health 22 (1996) 5–13.
[11] N. Ramirez, A.C. Lewis, R.M. Marce, F. Borrull, J.F. Hamilton, Environ. Int. 71 (2014) 139–147.
[12] L.M. Petrick, A. Svidovsky, Y. Dubowski, Environ. Sci. Technol. 45 (2011) 328–333.
[13] J. Repace, A. Lowrey, Science 208 (1980) 464–472.
[14] G. Banderali, A. Martelli, M. Landi, F. Moretti, F. Betti, G. Radaelli, C. Lassandro, E. Verduci, J. Transl. Med. 13 (2015) 327.
[15] N.E. Klepeis, W.C. Nelson, W.R. Ott, J.P. Robinson, A.M. Tsang, P. Switzer, J.V. Behar, S.C. Hern, W.H. Engelmann, J. Expo. Anal. Environ. Epidemiol. 11 (2001) 231–252.
[16] J. Spengler, K. Sexton, Science 221 (1983) 9–17.
[17] D.L. Hoffmann, C.D. Standish, M. García-Diez, P.B. Pettitt, J.A. Milton, J. Zilhão, J.J. Alcolea-González, P. Cantalejo-Duarte, H. Collado, R. de Balbín, M. Lorblanchet, J. Ramos-Muñoz, G.-Ch. Weniger, A.W.G. Pike, Science 359 (2018) 912–915.
[18] D.L. Hoffmann, D. Angelucci, J. Villaverde, E.V. Zapata, J. Zilhão, Sci. Adv. 4 (2018) eaar5255.
[19] P. Walter, L. de Viguerie, Nat. Mater. 17 (2018) 106–109.
[20] K. Nassau, Color Res. Appl. 12 (1987) 4–26.
[21] S. Kment, F. Riboni, S. Pausova, L. Wang, L. Wang, H. Han, Z. Hubicka, J. Krysa, P. Schmuki, R. Zboril, Chem. Soc. Rev. 46 (2017) 3716–3769.
[22] P. Yang, Z.-J. Zhao, X. Chang, R. Mu, S. Zha, G. Zhang, J. Gong, Angew. Chem. Int. Ed. 57 (2018) 7724.
[23] P. Chen, H. Wang, H. Liu, Z. Ni, J. Li, Y. Zhou, F. Dong, Appl. Catal. B 242 (2019) 19–30.
[24] J. Li, X. Dong, Y. Sun, G. Jiang, Y. Chu, S.C. Lee, F. Dong, Appl. Catal. B 239 (2018) 187–195.
[25] H. Tong, S. Ouyang, Y. Bi, N. Umezawa, M. Oshikiri, J. Ye, Adv. Mater. 24 (2012) 229–251.
[26] F. Dong, Z. Wang, Y. Li, W.K. Ho, S.C. Lee, Environ. Sci. Technol. 48 (2014) 10345–10353.
[27] A. Vohra, D.Y. Goswami, D.A. Deshpande, S.S. Block, Appl. Catal. B 64 (2006) 57–65.
[28] X. Lang, X. Chen, J. Zhao, Chem. Soc. Rev. 43 (2014) 473–486.
[29] Q. Liang, Z. Li, Z.-H. Huang, F. Kang, Q.-H. Yang, Adv. Funct. Mater. 25 (2015) 6885–6892.
[30] Z. Zhao, W. Zhang, X. Lv, Y. Sun, F. Dong, Y. Zhang, Environ. Sci.: Nano 3 (2016) 1306–1317.
[31] R. Wang, W. Zhang, W. Zhu, L. Yan, S. Li, K. Chen, N. Hu, Y. Suo, J. Wang, Chem. Eng. J. 348 (2018) 292–300.
[32] X. Liu, J. Iocozzia, Y. Wang, X. Cui, Y. Chen, S. Zhao, Z. Li, Z. Lin, Energy Environ. Sci. 10 (2017) 402–434.
[33] X. Chen, L. Liu, P.Y. Yu, S.S. Mao, Science 331 (2011) 746–750.
[34] G. Liu, L.-C. Yin, J. Wang, P. Niu, C. Zhen, Y. Xie, H.-M. Cheng, Energy Environ. Sci. 5 (2012) 9603–9610.
[35] M. Xiao, B. Luo, S. Wang, L. Wang, J. Energy Chem. 27 (2018) 1111–1123.
[36] S. Wang, T. Wang, W. Chen, T. Hori, Chem. Commun. 32 (2008) 3756–3758.
[37] X. Wang, W. Lu, Y. Chen, N. Li, Z. Zhu, G. Wang, W. Chen, Chem. Eng. J. 335 (2018) 82–93.
[38] E. Ju, K. Dong, Z. Chen, Z. Liu, C. Liu, Y. Huang, Z. Wang, F. Pu, J. Ren, X. Qu, Angew. Chem. Int. Ed. 55 (2016) 11467–11471.
[39] X. Chen, W. Lu, T. Xu, N. Li, D. Qin, Z. Zhu, G. Wang, W. Chen, Appl. Catal. B 201 (2017) 518–526.
[40] W. Lu, T. Xu, Y. Wang, H. Hu, N. Li, X. Jiang, W. Chen, Appl. Catal. B 180 (2016) 20–28.
[41] H. Liu, S. Bao, Z. Cai, T. Xu, N. Li, L. Wang, H. Chen, W. Lu, W. Chen, Chem. Eng. J. 317 (2017) 1092–1098.
[42] X. Zhang, L. Yu, C. Zhuang, T. Peng, R. Li, X. Li, ACS Catal. 4 (2014) 162–170.
[43] C. Zhang, R. Hao, H. Yin, F. Liu, Y. Hou, Nanoscale 4 (2012) 7326.
[44] X. She, J. Wu, H. Xu, J. Zhong, Y. Wang, Y. Song, K. Nie, Y. Liu, Y. Yang, M.T. Rodrigues, R. Vajtai, J. Lou, D. Du, H. Li, P.M. Ajayan, Adv. Energy Mater. 7 (2017) 1700025.
[45] X. Chen, W. Lu, T. Xu, N. Li, Z. Zhu, G. Wang, W. Chen, Chem. Eng. J. 328 (2017) 853–861.
[46] T.Y. Ma, Y. Tang, S. Dai, S.Z. Qiao, Small 10 (2014) 2382–2389.
[47] G. Liu, P. Niu, C. Sun, S. Smith, Z. Chen, G. Lu, H. Cheng, J. Am. Chem. Soc. 132 (2010) 11642–11648.
[48] Q. Lin, L. Li, S. Liang, M. Liu, J. Bi, L. Wu, Appl. Catal. B 163 (2015) 135–142.
[49] S. Cao, J. Low, J. Yu, M. Jaroniec, Adv. Mater. 27 (2015) 2150–2176.
[50] W. Li, D. Li, Y. Lin, P. Wang, W. Chen, X. Fu, Y. Shao, J. Phys. Chem. C 116 (2012) 3552–3560.
[51] J. Cao, B. Luo, H. Lin, B. Xu, S. Chen, Appl. Catal. B 111–112 (2012) 288–296.
[52] C. Chang, L. Zhu, S. Wang, X. Chu, L. Yue, ACS Appl. Mater. Interfaces 6 (2014) 5083–5093.
[53] F. Liang, Y. Zhu, Appl. Catal. B 180 (2016) 324–329.
[54] Y. Hong, Y. Jiang, C. Lia, W. Fan, X. Yan, M. Yan, W. Shi, Appl. Catal. B 180 (2016) 663–673.
[55] W. Cui, J. Li, W. Cen, Y. Sun, S.C. Lee, F. Dong, J. Catal. 352 (2017) 351–360.
[56] L. Lian, S. Yan, B. Yao, S.A. Chan, W. Song, Environ. Sci. Technol. 51 (2017) 11718–11730.
[57] H. Yu, H. Tang, X. Zhu, Y. Li, P. Xu, Appl. Environ. Microbiol. 81 (2015) 272–281.
[58] R. Brandsch, Appl. Mierobiol. Biotechnol. 69 (2006) 493–498.
[59] M. Kato, K. Sakai-Kato, T. Toyo'oka, J. Sep. Sci. 28 (2005) 1893–1908.